

Particle Dynamics in Sheared Granular Matter

W. Losert,¹ L. Bocquet,^{2,3} T. C. Lubensky,² and J. P. Gollub^{1,2}

¹*Physics Department, Haverford College, Haverford, Pennsylvania 19041*

²*Physics Department, University of Pennsylvania, Philadelphia, Pennsylvania 19104*

³*Laboratoire de Physique de l'E.N.S. de Lyon, U.M.R. C.N.R.S. 5672, 46 Allée d'Italie, 69364 Lyon Cedex, France*

(Received 21 April 2000)

The particle dynamics and shear forces of granular matter in a Couette geometry are determined experimentally. The normalized tangential velocity $V(y)$ declines strongly with distance y from the moving wall, independent of the shear rate and of the shear dynamics. Local rms velocity fluctuations $\delta V(y)$ scale with the local velocity gradient to the power 0.4 ± 0.05 . These results agree with a locally Newtonian, continuum model, where the granular medium is assumed to behave as a liquid with a local temperature $[\delta V(y)]^2$ and density dependent viscosity.

PACS numbers: 45.70.Mg, 47.50.+d, 83.70.Fn

An important property of granular matter is partial fluidization in response to shear stresses [1]. Stationary granular matter can sustain normal loads and shear stresses, but if a threshold shear stress is exceeded, part of the material starts to flow with properties that appear to differ from those of a Newtonian fluid. Unlike ordinary fluids, granular materials do not exhibit intrinsic thermal motion. Instead, the granular “temperature,” generally defined as the square of rms velocity fluctuations δV^2 , is created by the flow itself. As a result, the mean flow and rms fluctuations are related. This fundamental connection has been investigated experimentally [2] but remains poorly understood.

The forces generated in sheared granular matter were first investigated in the pioneering work of Bagnold [3] by confining the material in a Couette cell between a stationary outer cylinder and a rotating inner cylinder. Several recent experiments and simulations investigated individual particle motion in the same geometry [4–6]. These studies indicate that the mean particle velocity parallel to the shear direction $V(y)$ decreases faster than linearly away from the inner cylinder.

The velocity profile in three dimensions was determined by Mueth *et al.* [6]. Measurements were carried out both in the interior of the material using x-ray and NMR techniques, and on the bottom surface of the Couette cell by optical imaging. These measurements showed that the velocity profile on the bottom surface and in the interior are the same. $V(y)$ varies from nearly Gaussian for kidney shaped particles to roughly exponential for spherical particles. Layering of particles is suggested as the cause of this variation.

In previous studies in a planar geometry [7], we have found that most of the flow is confined to five to six layers of particles close to the shear plane. The mean particle velocities during brief slips of the shearing plate decrease roughly exponentially with distance away from the moving plate, consistent with the findings in the Couette geometry.

The aim of the present experiment is to understand the relationship among mean velocities, rms fluctuations, and

shear forces of a steady state shear flow. We have developed a locally Newtonian, continuum model that describes the granular medium as a liquid with nonuniform temperature and density dependent viscosity. The interplay between mean flow and rms velocity fluctuations can be understood quantitatively in this context, as we demonstrate.

In the experiments we shear the granular material in a Couette geometry. We measure both the mean particle velocities $V(y)$ and the velocity fluctuations $\delta V(y)$ on the upper surface of the granular material. These should approximate particle motion in the interior based on the previous 3D measurements described above [6].

In the experimental apparatus the granular material (0.75 mm diameter black glass beads) is confined to a 12 mm gap between a stationary outer cylinder and a rotating inner cylinder ($r = 51$ mm), as shown in Fig. 1. The inner cylinder is hollow to reduce its inertia and is coated with a monolayer of randomly packed glass beads. The outer cylinder is made of glass and is coated with a monolayer of randomly packed glass beads up to the height of the top surface, which allows observation of the top layer of grains through a mirror as shown in Fig. 1. To shear the material, the inner cylinder is rotated at a variable rate of 0.001–1 Hz. The lower 38 mm of the inner cylinder is stationary in order to minimize boundary layer effects.

The inner cylinder is connected to a microstepping motor via a flexible tempered steel spring. The spring bending is proportional to the applied shear force. We measure the spring displacement with a capacitive displacement sensor that is rigidly connected to the motor shaft. This spring configuration allows us to measure instantaneous shear forces with excellent dynamic range and precision and permits both stick-slip dynamics and continuous motion of the inner cylinder, depending on parameters. The trajectories of roughly 100 individual particles in the surface layer are determined with a fast charge coupled device (CCD) camera at 30–1000 frames/sec. Particle motion is extracted from sequences of 2000 images with a spatial resolution

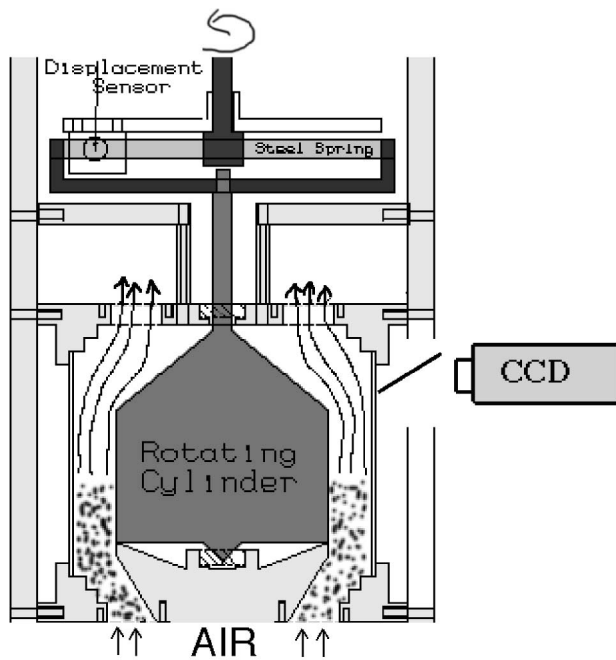


FIG. 1. Experimental setup: The granular material (between two concentric cylinders) is fluidized by an upward air flow and sheared by rotation of the inner cylinder, which is connected to the motor through a flexible spring (S). Shear forces are determined from the spring displacement. Particle motions in the top layer are measured through the glass outer cylinder with a fast CCD camera.

of <0.1 pixels. From the particle tracks we determine average particle velocities $V(y)$ and rms velocity fluctuations $\delta V(y)$ as a function of distance y from the rotating inner cylinder.

The shear dynamics are found to be very similar to the dynamics of a plate sliding across a granular layer [8]. At low shear rates the motion of the inner cylinder is intermittent with short, rapid slips, and long periods of sticking. At sufficiently high shear rates (or with a stiff spring), steady motion of the inner cylinder is observed.

We can also apply an upward air flow at a variable rate through the granular material. Air flow reduces the shear forces, as already noted by Tardos *et al.* [9], and it also suppresses stick-slip motion. Without air flow, stick-slip motion is observed with a mean shear force of 95 N/m^2 . At a mean air flow speed of $\sim 1.6 \text{ m/s}$ through the granular material, shear forces are reduced by a factor of 4 and steady sliding motion is observed. To measure $V(y)$ and $\delta V(y)$ in the steady sliding regime, most experiments described below were carried out at large air flow just below the threshold of the “bubbling” instability. (The air flow does not produce velocity fluctuations in the absence of shear.) We have also suppressed the stick-slip motion using a rigid drive connection without air flow. Both $V(y)$ and $\delta V(y)$ remain unchanged [10].

Measurements of shear forces, analyzed in the context of our hydrodynamic model, will be presented elsewhere

[10]. Here we note that the mean shear stress does not change with shear rate over more than 2 orders of magnitude in the shear rate. This behavior may be contrasted to the quadratic increase of shear stress with the shear rate observed in Ref. [3], where the material was immersed in a fluid and kept at constant volume.

The average velocity of particles at the surface of the shear cell is shown in Fig. 2 as a function of distance y from the rotating inner cylinder, for inner wall velocities U ranging from 0.004 to 0.4 Hz. As found previously, the velocity profile decays strongly to zero over a few particle diameters d . The normalized velocity profile is independent of the imposed shear rate over at least 2 orders of magnitude in shear rate. We also find that without air flow (at $U = 0.01 \text{ Hz}$, solid triangles), the inner cylinder moves with stick-slip dynamics rather than steady sliding, but the velocity profile remains unchanged.

Figure 3 shows the rms velocity fluctuations, which have not been previously measured in a 3D system. The fluctuations are slightly larger in the direction parallel to the mean flow than perpendicular to it. Since parallel fluctuations would also include the effect of fluctuations in the mean flow, we show only the perpendicular fluctuations. The velocity fluctuations decrease roughly exponentially far from the inner cylinder. However, the fluctuations decrease more slowly with y than does the average velocity.

The rms fluctuation is the key quantity in a flowing granular material. As already proposed by Reynolds [11], the system has to dilate in order to allow flow, which implies particle motion transverse to the flow direction. This

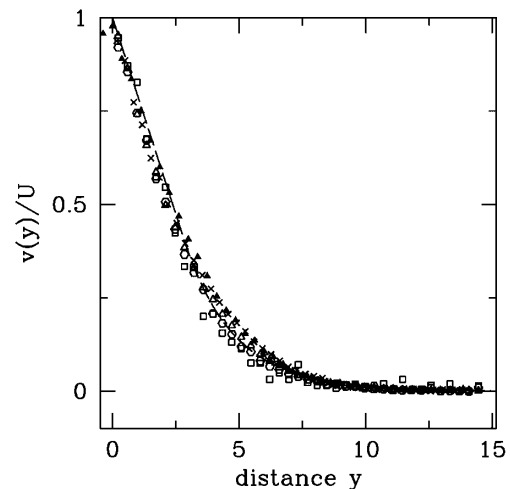


FIG. 2. Mean particle velocity (normalized by the shear rate) as a function of distance from the inner cylinder (in particle diameters). The respective shear rates U (in Hz) are 0.004 (hexagons), 0.04 (squares), 0.01 (open triangles), 0.4 (crosses). The solid triangle is the velocity profile at $U = 0.01 \text{ Hz}$ without air flow. The normalized velocity profile is independent of shear rate and shear dynamics (intermittent or steady motion). The dashed line is the solution of Eqs. (2) and (3), with $\delta = 4.7d$, $y_w = 2.8d$, and $\alpha = 0.4$ (see text for details).

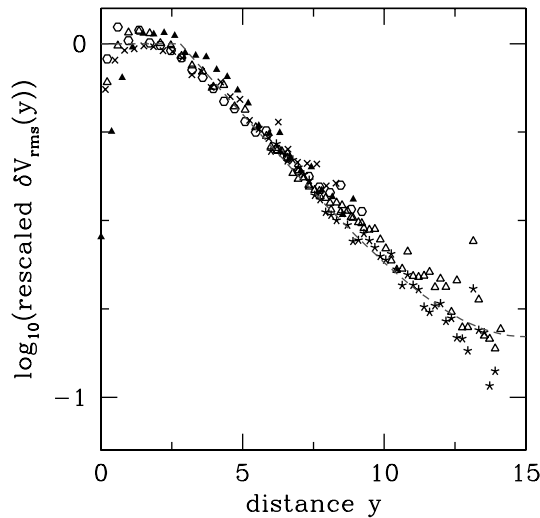


FIG. 3. rms velocity fluctuations perpendicular to the shear direction. Fluctuations decrease roughly exponentially far from the inner cylinder, but more slowly than the mean flow. The rms fluctuations are rescaled (shifted vertically) such that all experimental points fit on the same master curve. The dashed line is the theoretical result (see text), with a decay length $\delta = 4.7d$ and a boundary position $y_w = 2.8d$.

transverse motion vanishes on average and, therefore, its rms fluctuations contain the physically relevant information characterizing the flow properties.

In a phenomenological description, it is tempting to consider these rms velocity fluctuations as an effective *granular temperature* and consider a *local* hydrodynamic model as a starting point, as has already been proposed in the literature (see, e.g., [12]). Within such a picture the granular temperature obeys a transport equation characterizing the balance between “heat flow” and dissipation due to the inelastic collisions:

$$\partial_y \lambda \partial_y T - \epsilon T = 0. \quad (1)$$

(Note that a local heating term has been omitted, which can be shown to be valid far from the moving boundary.)

This *local* equation introduces two transport coefficients, the thermal conductivity λ and the energy loss rate ϵ . Both λ and ϵ are proportional to the collision frequency. In the high density limit we consider, $\rho \sim \rho_c$ with ρ_c the density at random close packing, λ and ϵ are proportional to $P/T^{1/2}$, where P is the isotropic pressure [12]. Stress conservation in the y direction implies that P is constant over the cell. From Eq. (1), one can obtain the temperature profile as

$$T^{1/2}(y) = T_0^{1/2} \frac{\cosh[(H-y)/\delta]}{\cosh(H/\delta)}, \quad (2)$$

where δ , defined as $\delta^2 = 2\lambda/\epsilon$, is proportional to the bead diameter d , and is independent of position and temperature. A vanishing heat flux has been assumed at the outer stationary boundary in agreement with additional experimental measurements for wider shear regions, while the

temperature at the moving boundary, T_0 , is introduced as a boundary condition at the wall. T_0 is created by the flow in the first layers close to the wall, so that Eq. (1) is assumed to apply only for distance y larger than a cutoff distance y_w from the wall: y_w quantifies the width of the boundary layer in which temperature is created by the motion of the inner cylinder. The fit to experimental data yields $y_w = 2.8d$. The effective cell width H is thus $H_0 - y_w$, where H_0 is the wall to wall distance. As shown in Fig. 3, this hydrodynamic model shows good agreement with the experimental data.

Within the framework of this phenomenological model, the velocity profile can be constructed from the constant shear-rate condition, $\sigma_{xy} = \eta \dot{\gamma} = \text{const}$ independent of y , with $\dot{\gamma} = dV_x(y)/dy$ the local shear rate and η the viscosity. The viscosity is expected to scale with the collision frequency, $\eta = \eta_0 P / (\rho_c d^2 T^{1/2})$ (where d is the bead diameter, η_0 is a dimensionless number, and $\rho \sim \rho_c$ has been assumed), so that the local shear rate obeys $T^{1/2} = \eta_0 P / (\rho_c d^2 \sigma_{xy}) \dot{\gamma}$. This local relationship can be compared to the experimental data by plotting the local rms velocity as a function of the local velocity gradient $\dot{\gamma}$. As shown in Fig. 4, a remarkable scaling relationship is found between these two local quantities,

$$\delta V_{\text{rms}} \equiv T^{1/2} \sim \dot{\gamma}^\alpha \quad (3)$$

with an exponent $\alpha \approx 0.4$. This scaling behavior is not in agreement with the simple scaling of the viscosity with the collision frequency only, for which an exponent of 1 would have been measured.

The actual scaling can be understood if we assume that the dimensionless coefficient η_0 contains an additional contribution that diverges algebraically, when the density reaches random close packing, ρ_c , i.e., $\eta_0 = \tilde{\eta}_0 (1 - \rho/\rho_c)^{-\beta}$. The density can be related to the granular

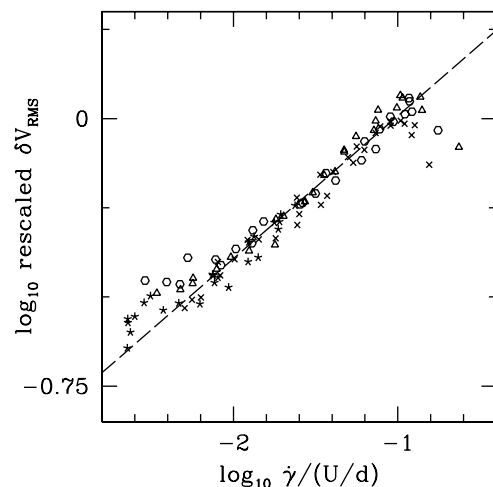


FIG. 4. Connection between the local rms velocity fluctuations and local shear rate (same symbols as for Fig. 2). Local fluctuations are found to increase approximately as a power law of the local velocity gradient, with a power of 0.4 (dashed line).

temperature through the constant isotropic pressure P , which can be formally written as $P = \rho f(\rho)T$. The dimensionless function $f(\rho)$ is expected to diverge like $(1 - \rho/\rho_c)^{-1}$ at random close packing [12], so that at constant pressure P , in a region where $\rho \sim \rho_c$, one has $\rho_c - \rho \sim T$. Note that this relation is consistent with Reynolds' remark that the density has to decrease in order to allow flow, which occurs for nonzero granular temperature. Together with the constant shear rate condition, these relations imply a nonlinear algebraic scaling of $\delta V(y)$ with the shear rate, with an exponent $\alpha = (2\beta + 1)^{-1}$. With the experimentally determined exponent $\alpha = 0.4$, we obtain the overall divergence of the viscosity with density as $\eta \sim (\rho_c - \rho)^{-1.75}$.

Using the previously obtained temperature profile, Eq. (3) can be integrated (with no-slip boundary conditions at both walls) to give the velocity profile. The corresponding result is plotted in Fig. 2 as a dashed line, indicating good agreement with the experimental profile.

Finally, we measure granular flow when the gap between the two cylinders is only 5 particle diameters wide.

In this case, the inner cylinder jams and can be moved only at high air flow rates and high rotation rates. For the narrow gap we find that $V(y)$ decreases linearly with y and that $\delta V(y)$ is uniform across the gap at shear rates of 0.1 and 0.02 rev/sec. This result is consistent with our model: A linear velocity profile is expected for a constant granular temperature. A constant granular temperature in turn is expected for cell widths smaller than the previously defined decay length δ .

The success of the present *local Newtonian hydrodynamic* model in describing the experimental data (even for small driving velocities) calls for a deeper understanding. The basic ingredient of the present model is the algebraically diverging viscosity close to random close packing. In a granular material, the ability to flow relies mainly on a decrease in the local density. Such a decrease can be caused by the onset of rms velocity fluctuations. Lowering the density allows some particles to move, creating "fluidized regions," while other regions remain in clusters at rest. The flow properties can be thus formulated in terms of the local fluidization probability, or cluster lifetime. In a granular material, these quantities might be estimated by means of a free volume estimate, along the lines proposed by Edwards and Grinev [13] for granular matter and earlier by Cohen and Turnbull [14] in the context of transport in glassy systems. These models predict a very strong divergence of the viscosity close to random close packing, in qualitative agreement with the present results. More precisely, our data are consistent with an algebraic divergence, which is also expected in supercooled liquids when the density approaches the critical density [15].

The model quantitatively describes all major aspects of the experimental results: (i) The rms velocity fluctuations increase with the local shear rate to a given power. (ii) The velocity decreases strongly away from the moving

wall. (iii) The normalized velocity profile is independent of shear rate and shear dynamics. A detailed comparison between our experimental results and our model, including a description of the influence of air flow and shear rate on shear forces and T_0 , will be published elsewhere [10].

More generally, our experimental results indicate that there may be a useful analogy between the dynamics of granular materials and the behavior of supercooled liquids close to the glass transition. Such an analogy was proposed in a recent paper by Liu and Nagel [16]. Our results support this conjecture and indicate the quantitative relationship: The flow properties reported here are quantitatively predicted from a locally Newtonian, continuum model, provided that the local temperature is identified with $(\delta V)^2$ and that the viscosity is assumed to diverge as the density approaches a critical value. The specific properties of individual particles enter only through the few adjustable parameters of the model. Once determined in a specific geometry, the flow properties in any geometry can be predicted. Further experiments are under way to verify this predictive power of the model.

We thank A. Liu, H. Jaeger, and C. Bizon for helpful discussions. This work was supported by the National Science Foundation under Grants No. DMR-9704301, No. DMR-9730405, and No. DMR-9632598.

-
- [1] H. M. Jaeger, S. R. Nagel, and R. P. Behringer, *Rev. Mod. Phys.* **68**, 1259 (1996).
 - [2] N. Menon and D. J. Durian, *Science* **275**, 1920 (1997).
 - [3] R. A. Bagnold, *Proc. R. Soc. London A* **225**, 49 (1954); **295**, 219 (1966).
 - [4] S. Schöllmann, *Phys. Rev. E* **59**, 889 (1999).
 - [5] C. Veje *et al.*, in *Physics of Dry Granular Media*, edited by H. J. Herrmann, J. P. Hovi, and S. Luding, NATO ASI Ser. E, Vol. 350 (Kluwer, Dordrecht, 1998).
 - [6] D. M. Mueth *et al.*, cond-mat/0003433.
 - [7] W. Losert, J.-C. Géminard, S. Nasuno, and J. B. Gollub, *Phys. Rev. E* **61**, 4060 (2000).
 - [8] S. Nasuno, A. Kudrolli, and J. P. Gollub, *Phys. Rev. Lett.* **79**, 949 (1997).
 - [9] G. I. Tardos, M. I. Khan, and D. G. Schaeffer, *Phys. Fluids* **10**, 335 (1998).
 - [10] L. Bocquet, W. Losert, T. C. Lubensky, and J. P. Gollub (unpublished).
 - [11] O. Reynolds, *Philos. Mag.* **20**, 469 (1885).
 - [12] J. T. Jenkins and S. B. Savage, *J. Fluid Mech.* **130**, 186 (1983); P. K. Haft, *J. Fluid Mech.* **134**, 401 (1983). Our model extends this work by introducing a stronger divergence of viscosity with density.
 - [13] S. F. Edwards and D. V. Grinev, *Phys. Rev. E* **58**, 4758 (1998).
 - [14] M. H. Cohen and D. Turnbull, *J. Chem. Phys.* **31**, 1164 (1959).
 - [15] W. Gotze and L. Sjogren, *Rep. Prog. Phys.* **55**, 241 (1992).
 - [16] A. J. Liu and S. R. Nagel, *Nature (London)* **396**, 21 (1998).